A NOVEL DECONVOLUTION ALGORITHM FOR IMAGE RESTORATION

Phu Ninh Tran[1], Quang Thi Nguyen[2], Hieu Dang Quang[2], Hong Quang Le[3]
[1]Faculty of Radio-electronic, Le Quy Don Technical University, Ha Noi, Vietnam
[2]Integrated System Institute, Le Quy Don Technical University, Ha Noi, Vietnam
[3]Faculty of Missile and Artillery, Naval Academy, Nha Trang, Vietnam

ABSTRACT
A novel deconvolution algorithm for restoring blurred image is introduced. The proposed algorithm can behave two multi-scale frameworks to restore the fuzzy blurred image. One multi-scale framework is used to optimize whole process containing kernel estimation and deconvolution by incorporating an average difference criterion for evaluating the restored image quality, another is applied to optimize kernel estimation process, which are generated kernels in different sizes. Furthermore, the Expectation Maximization (EM) method is applied to handle outliers in deconvolution process for suppressing ringing effects. The experimental result shows that the proposed method offers an efficient way to estimate and optimize the blur kernel and obtain good results for deconvolution process.

KEYWORDS: *Camera Shake; Blind Deconvolution; Blur Kernel; Kernel Estimation, Multi-scale*

I. INTRODUCTION

Camera shake during exposure can generate the blur image. Much significant progress has been made recently towards removing this blur from images. However, in recent literature, the kernel size is usually evaluated manually in kernel estimation and some unsatisfactory influences caused by outliers are not noticeable in the deblurring process.

The kernel size in deconvolution has significant influence in image quality but there is no guidance on how to find the optimal size for kernel in previous works. A multi-scale approach is introduced by Fergus et al. [7], which perform kernel estimation by varying image resolution in a coarse to fine method. However, there are no criteria for evaluating the size of kernel and it must be approximated manually from user. Hence, the effectiveness of that method depend on the selection of kernel size. Levin et al. [12] further demonstrate that a MAP estimation of kernel alone is well constrained and produces a good result, while a simultaneous MAP estimation of both latent image and blur kernel fail. Their evaluation of current algorithms suggests that the variational Bayesian approach within multi-scale estimation (Fergus et al. [7]), a good MAP_k estimator outperforms other existing methods. However, it has been noted that when the kernel is quite large (i.e. 30 x 30 pixels or larger), the kernel estimation by variational Bayesian approach is inaccurate and unreliable. Harmeling et al. [9] proposed a multi-scale deconvolution algorithm to constrain the MAP solution to the desired one from coarse to fine. The multi-scale initialization and the iterative likelihood update are further adopted to ensure that the optimization converges at the desired local minimum. By doing so, authors are able to restore high quality results, especially from ones with large blur kernel but there is still some residually ringing that is unavoidable due to frequency loss during blurring.

Furthermore, many blind deconvolution methods, which have been described in previous works have not considered the outliers such as pixel saturation, non-Gaussian noise and nonlinear camera response curve that cause severe ringing artifacts in final output images. A natural image statistics combine with L2-norm based data fidelity term is proposed by Shan et al. [14], that can obtain accurate results but this method only behaves in case that observed image contain a small amount of

noise. The saturation correction method (Harmeling et al., [9]), which handling saturated pixels by thresholding input observed images leads to better reconstructions but the author does not deal with threshold value optimization. Yuan et al. [15] tries to handle outliers by using a coarse-to-fine progressive deconvolution approach. This method can suppress ringing artifacts but still have disadvantages in output image. Cho, S. et al. [3] demonstrated that outliers violate the linear blur assumption and consequently cause severe ringing artifacts to the result image. It is inappropriate to use a linear blur model when outliers exist, so it is necessary to avoid the violation of outliers. Unfortunately, most sources of the outliers are inevitable. The method that masks out the outliers, Harmeling et al. [9], involves a threshold which distinguishes the outliers for masking out. However, there is no guidance on how to find the optimal threshold value, so that method is not robust enough.
In this paper, a blind deconvolution algorithm for removing camera shake effects, which apply two multi-scale frameworks to restore the shaken image is proposed. One multi-scale framework is to optimize the whole process containing kernel estimation and deconvolution by incorporating an average difference criterion for evaluating the restored image quality, another one is to optimize kernel estimation, which are generated kernels in different sizes. Especially, the Expectation Maximization (EM) method is applied to handle outliers in deconvolution process for suppressing ringing effects.

II. MATERIALS AND METHODS

To solve above-mentioned problems, in this paper, a new method for restoring the latent image from camera shake blur image is proposed by exploiting recent research in natural image statistics and obtained the improvement in experimental results. An algorithm is developed that explicitly handles outlier combine with an average difference criterion for estimating the blur kernel in the deconvolution process. A global multi-scale approach is used in blind restoration and some useful information in outlier modeling is exploited for effective reconstruction of the latent image. Fig. 1 shows the procedure of our restoration method.

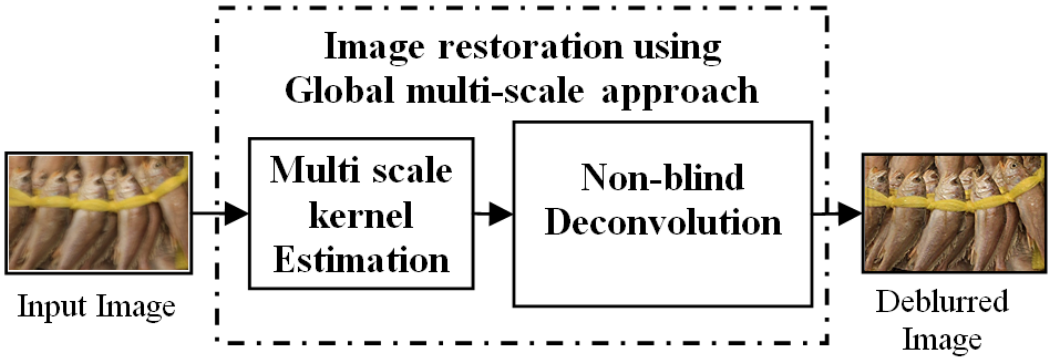

Figure 1. The procedure of restoration

2.1. Kernel Estimation

Camera shake image restoration is typically addressed by first estimating the kernel, and then estimating the sharp image when the kernel is obtained. This method is not an exception. The blur model can represent a blurred image *b* as a convolution of the latent image *l* with a blur kernel *k* plus additional image noise *n*:

$$b = k \otimes l + n \tag{1}$$

where $\otimes$ is the convolution operator and *n* denotes sensor noise at each pixel. The problem of blind-deconvolution is to recover the latent image *l* from blurred image *b* without specific knowledge of blur kernel *k*.
According to (1), given blurred image *b*, the posterior distribution is presented with Bayes' rule:

$$p(k, \nabla l \mid \nabla b) \quad \propto \quad p(\nabla b \mid k, \nabla l)\, p(k)\, p(\nabla l) \tag{2}$$

where ∇ denotes the gradient operator, k is blur kernel, ∇l is latent image gradient and ∇b is blur image gradient.

A common technique for solving (2) is using maximum a posteriori (MAP) approach, which maximizes $p(k,\nabla l|\nabla b)$ by finding the kernel k and ∇l. However, the MAP objective function is very susceptible to poor local minima. Therefore, our purpose is to approximate the full posterior distribution $p(k,\nabla l|\nabla b)$ and then estimate the kernel k with maximum marginal probability. The kernel is selected that is most likely with respect to the distribution of possible latent images, thus avoiding the over-fitting that can occur when selecting a single "best" estimate of the image.

In order to reduce the ringing artifacts during latent image restoration and the ill-posed of the deconvolution problem, we use the latent image prior $p(\nabla l)$, which defined as:

$$p(\nabla l)=\prod_i e^{\phi(\partial\nabla l_i)} \tag{3}$$

where i indexes over image pixels, ∂ denotes the partial derivative, $\Phi(\partial\nabla l_i)$ is represented as:

$$\Phi(\nabla\partial l_i)=\begin{cases}-k\left|(\nabla\partial l_i)\right|^2 & if \quad \nabla\partial l_i \le p_t \\ -\left(a(\nabla\partial l_i)^2+b\right) & otherwise\end{cases} \tag{4}$$

where k, a, b are the curve fitting parameters while $-\left(a(\nabla\partial l_i)^2+b\right)$ models the heavy tails of distribution, p_t indexes the position which the two functions are concatenated.

The natural image statistics have been shown that the kernel prior obey heavy-tailed distributions in their gradients. The zero values in the kernel are encouraged by incorporating sparsity prior $p(k)$, which is defined as:

$$p(k)=\prod_j\sum_{d=1}^{D}\pi_d E(k_j\mid\lambda_d) \tag{5}$$

where j indexes over blur kernel elements, D denotes exponential distribution with scale factors λ_d and weights π_d for the d-th component, E denotes exponential distribution. D = 4 were used in our experiment.

Combination of (3) and (5) with assuming the plus noise is Gaussian can obtain:

$$p(\nabla b\mid k,\nabla l)=\prod_i N(\nabla b_i\mid k\otimes\nabla l_i,\sigma^2) \tag{6}$$

where i indexes over image pixels, N is Gaussian distribution, σ^2 is unknown noise variance.

For solving Eq.(2) using variational Bayesian approach, apply Kullback-Leibler divergence to measure distance between the approximating distribution $q(k|\nabla l)$ and the true posterior $p(k,\nabla l|\nabla b)$, and the cost function C_{KL} is defined as:

$$\begin{aligned}C_{KL}&=KL\left\{q(k,\nabla l,\sigma^2)\,\|\,p(k,\nabla l|\nabla b)\right\}-\ln p(\nabla b)\\&=\int q(\nabla l)\ln\frac{q(\nabla l)}{p(\nabla l)}d\nabla l+\int q(k)\ln\frac{q(k)}{p(k)}dk+\int q(-\sigma^2)\ln\frac{q(-\sigma^2)}{p(-\sigma^2)}d(-\sigma^2)\end{aligned} \tag{7}$$

Because σ^2 is unknown, $q(k,\nabla l,\sigma^2)$ is used to represent $q(k,\nabla l)$. Minimize Eq.(7) by using iterative method based on variational Bayesian expectation maximization rule, the blur kernel can be estimated.

To perform kernel estimation using coarse to fine method, we build a multi-scale pyramids for both images and kernels. For the coarsest level, we set kernel size as 3 x 3 pixels, and each level can be generated by up-sampling the previous level by factor $\sqrt{2}$. From coarse to fine, our method progressively suppresses noise and weak image edges that are less helpful to kernel estimation, while still maintaining main image structures and strong edges. The image size of the coarsest scale

corresponding to the 3x3 kernel is smaller than our minimum practical size, so we only down-sample the blurred image until is reaches 128x128, and initialize the kernel extracted from a point light source trajectory perturbed by a simple user-drawn line (show in Fig. 2(e)). Our approach produces a visually pleasant result even comparable to double image deconvolution method (Yuan et al., 2007), as show in Fig. 2.

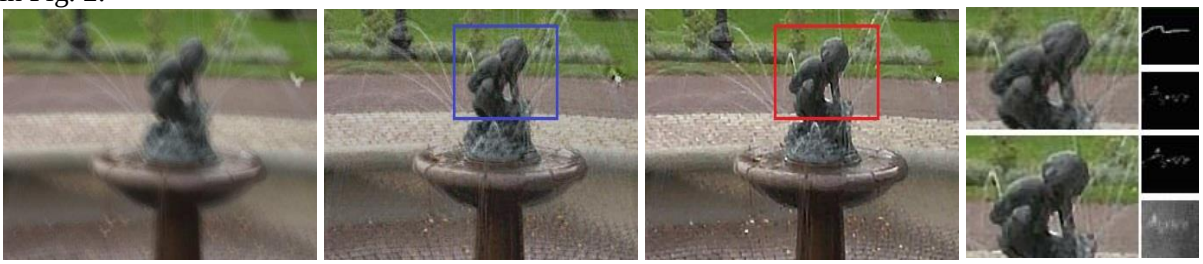

(a) **(b)** **(c)** **(d)** **(e)**

Figure 2. (a) Blurred image, (b) Result by Yuan et al's two image deblurring method, (c) Our result, (d) Closed-up patches, (e) From up to down: the user-drawn line, our final kernel, the kernel by Yuan et al's two image method and the trajectory in the blurred image.

2.2. Reference Image Estimation

After obtaining estimated and fixed the kernel, the final shape image is recovered by combination of fast image deconvolution using hyper-Laplacian priors [19] and the model of the spatially random distribution of image noise [14]. According to the fast image deconvolution using hyper-Laplacian priors, the latent image can be estimated very quickly with following equations.

$$\begin{aligned} I^* &= \min_I \sum_{i=1}^{N} \left(\frac{\lambda}{2}(I \otimes K - B)_i^2 + \sum_{j=1}^{2} |(I \otimes f_j)_i|^{\alpha}\right) \\ &= \min_{I,w} \sum_{i=1}^{N} \left(\frac{\lambda}{2}(I \otimes K - B)_i^2 + \frac{\beta}{2}(\|(I \otimes f_1)_i - w_i^1\|_2^2 + \|(I \otimes f_2)_i - w_i^2\|_2^2)\right. \\ &\left. + |w_i^1|^{\alpha} + |w_i^2|^{\alpha}\right) \end{aligned} \tag{8}$$

Where I^* is the estimated latent image, i is the pixel index, f_1 and f_2 are two first order derivative filters, $f_1 = [1 \ \ -1]$, $f_1 = [1 \ \ -1]^T$, β is a weight that wil be varied during the optimization, w_i^1 and w_i^2 (together denoted as w) are auxiliary variables that allow the term $(i \otimes f_j)_i$ to be moved outside the $|.|^{\alpha}$ expression. The model of the spatially random distribution of image noise sates that noise, $N = B - I \otimes P$, follows Gaussian with different standard distributions as follows [14].

$$p(B \mid I) = \prod_{\partial^* \in \Theta} \prod_i N(\partial^* B_i \mid \partial^* (I \otimes K)_i, \sigma_q^2) \tag{9}$$

where ∂^* denotes the operator of any partial derivative with $k(\partial^*) = q$ representing its order. $\partial^* N = \partial^*(B - I \otimes P)$ follows a Gaussian distributions with standard deviation $\sigma_q = \sqrt{2^q}\sigma_0$ where σ_0 denotes the standard deviation of N. $\Theta = \{\partial_0, \partial_x, \partial_y, \partial_{xx}, \partial_{xy}, \partial_{yy}\}$ represents a set of partial derivative operators [14].

The reference image is generated by combining (8) and (9) as follows.

$$\begin{aligned} I^* &= \min_{I,w} \sum_{i=1}^{N} \left(\frac{\lambda}{2}\left(\sum_{\partial^* \in \Theta} \tau_{k(\partial^*)} \|(\partial^* I \otimes K - \partial^* B)_i\|^2\right)\right. \\ &\left. + \frac{\beta}{2}(\|(I \otimes f_1)_i - w_i^1\|^2 + \|(I \otimes f_2)_i - w_i^2\|^2) + |w_i^1|^{\alpha} + |w_i^2|^{\alpha}\right) \end{aligned} \tag{10}$$

where $\tau_{k(\partial^*)} = 1, \ 0.5 \ \ and \ \ 0.25$ when $k(\partial^*) = 0, \ 1 \ \ and \ \ 2$ respectively. The combination of fast image deconvolution using hyper-Laplacian priors and the model of the spatially random distribution of image noise provides a powerful tool to estimate reference image. To solve (10),

$w = \{w_1, w_2\}$ values are calculated first with the method introduced in [19], and the reference image I^* is estimated with (11) given a fixed value of w.

$$\begin{aligned}&\left\{\frac{\beta}{\lambda}(F^{1^T}F^1 + F^{2^T}F^2) + K^T K + 0.5((F^1 C_K)^T F^1 C_K + (F^2 C_K)^T F^2 C_K)\right.\\&+0.25((F^1F^1C_K)^T F^1F^1C_K + (F^2F^2C_K)^T F^2F^2C_K + (F^2F^1C_K)^T F^2F^1C_K)\}i\\&=\left\{\frac{\beta}{\lambda}(F^{1^T}w^1 + F^{2^T}w^2) + C_K^T b + 0.5((F^1C_K)^T F^1 b + (F^2C_K)^T F^2 b)\right.\\&+0.25((F^1F^1C_K)^T F^1F^1 b + (F^2F^2C_K)^T F^2F^2 b + (F^2F^1C_K)^T F^2F^1 b))\}\end{aligned} \tag{11}$$

where i and b are the vetors forms of I and B respectively, $F^j i = f_j \otimes I$, and $C_K i = K \otimes I$.

2.3. Adaptive Regularization

The reference image indicates smoothed region and textured region better than the blurred image, but it still has small ringing artifacts and its image details are over smoothed. Thus, we regularize the image with regularization weighting factor that is changed according to the region based on the edge information from the reference image.

At first, a shock filter is used to restore edges in the reference image. A shock filter is an effective filter to recover sharp edges from blurred step signals [20]. The evolution equation of a shock filter is as follows.

$$I_{t+1} = I_t - sign(\nabla^2 I_t) \| \nabla I_t \| dt \tag{12}$$

where I_t is an image at time t, and ∇^2 and ∇ are the Laplacian and gradient, respectively. *dt* is the time step for a single evolution. After restoring edges with the shock filter, the edge information is extracted from the shock-filtered image. A 3 x 3 window is centered on a pixel in the shock-filtered image, and edge strength on the pixel is calculated as follows.

$$Eg(i,j) = \frac{\sum_{i,j} W_x(i,j) + \sum_{i,j} W_y(i,j)}{n} \tag{13}$$

where $Eg(i,j)$ is the edge strength at the pixel location, (i,j), $W_x = W \otimes [1 \ \ -1]$, $W_y = W \otimes [1 \ \ -1]^T$, W is the 3 x 3 window. The noise Eg is removed by thresholding. The threshold value is 5% of maximum of Eg. Based on this edge information of the reference image, we formulate the deconvolution problem as follows.

Arccording to Bayes framework, the posteriori for the latent image is written as:

$$p(I \mid B) \propto p(B \mid I) p(I) \tag{14}$$

where $p(B \mid I)$ denotes the likehood of blurred image given the latent image, and $p(I)$ represents the image prior. The maximum a posterori (MAP) solution of I can be obtained by minimizing the following energy:

$$I^* = \underset{I}{argmin}\, E(I) \tag{15}$$

where

$$E(I) = -log\ p(I \mid B) = -log\ p(B \mid I) - \log p(I) \tag{16}$$

The likelihood is based on noise, $N = B - I \otimes K$. For this likelihood, we adopt the model of the spatially random distribution of image noise [14] that is described in (9).

We also adopt the sparse distribution as the image prior [21]:

$$P(I) = exp\left(-\alpha(|\, I \otimes f_1\,|^{0.8} + |\, I \otimes f_2\,|^{0.8})\right) \tag{17}$$

where $f_1 = [1 \ \ -1]$ and $f_2 = [1 \ \ -1]^T$.

By taking the likelihood and prior into (18), we get

$$E(I)=\sum_{\partial^*\in\Theta}\tau_{k(\partial^*)}\,\|\,(\partial^* I\otimes K-\partial^* B)_i\,\|^2+\eta\,(|\,I\otimes f_1\,|^{0.8}+|\,I\otimes f_2\,|^{0.8}) \quad (18)$$

where $\eta=2\sigma_0^2\alpha$. Here, η is the regularization weighting factor that controls the strength of regularization and we use η=0.003 for the experiments. For adaptive regularization, we change the above equation to:

$$E(I)=\sum_{\partial^*\in\Theta}\tau_{k(\partial^*)}\,\|\,(\partial^* I\otimes K-\partial^* B)_i\,\|^2+\eta\,exp(-\frac{|\,Eg\,|^2}{\sigma_e})(|\,I\otimes f_1\,|^{0.8}+|\,I\otimes f_2\,|^{0.8}) \quad (19)$$

where Eg is the edge strength on the pixel of the reference image calculated with (13), and σ_e is the constant determining the shape of Gaussian function. We use $\sigma_e=1\times10^3$ by default. Thus, the effect of the regularization weighting factor, η, on the pixel is controlled according to $\exp\left(-|Eg|^2/\sigma_e\right)$.

To solve this equation, iterative re-weighted least squares (IRLS) algorithm is used. IRLS poses the optimization as a sequence of least squares problems, while each least square problem re-weighted by solution at the previous step [21]. Ringing artifacts are suppressed more and image details are preserved better in the adaptively regularized image than the reference image. Furthermore, we can obtain better results by setting this regularized image as the second reference image. The second reference image is shock-filtered, edge information is extracted, and adaptive regularization is applied to the blurred image again. This procedure can be repeated for better results, but we confirmed that two steps are enough for the good result.

Although the adaptively regularized image shows well preserved edges and reduced ringing artifacts, its fine scale detail layer is suppressed. This detail layer is enhanced as follows. If we define the adaptively regularized image as I_a, then the fine scale detail layer is obtained by subtraction the bilateral filtered I_a from I_a .Bilateral filter is defined as:

$$F\left(I\left(x\right)\right)=\frac{1}{Z_x}\sum_{x'\in W(x)}G_d(x-x')Gr\left(I(x)-I(x')\right)I(x') \quad (20)$$

where G_d and G_r are Gaussian function, $W\left(x\right)$ is a neighboring window and Z_x is a normalization term. This detail layer, $I_a-F\left(I_a\right)$, is added to the adaptively regularized image to obtain the final deconvolved image.

2.4. Multi-scale approach

In proposed method for kernel estimation and deconvolution, the kernel and deblurred image are obtained from the input blur image but we don't know which size of kernel is better, and when output deblurred image will reach the desired quality. This is also an ill-posed problem in recent research about blind deconvolution. The quality of output image depends on size of kernel. The optimal size of kernel (corresponding to the best quality of image) is different in each blur image. Hence, we propose a global multi-scale method for optimizing the kernel by estimating the average difference parameters. This parameter is used because it is simple to calculate, have a clear physical meaning, and is mathematically convenient in the context of optimization.

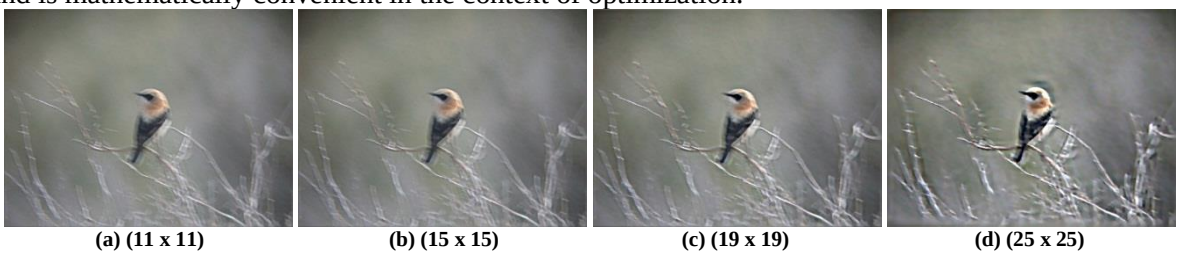

(a) (11 x 11) **(b) (15 x 15)** **(c) (19 x 19)** **(d) (25 x 25)**

Figure 3. Experimental Results with different size of kernels

The Average Difference parameter (AD) is used for estimating output image:

$$AD = \left| \sum_{j=1}^{M} \sum_{k=1}^{N} \left(x_{j,k} - x'_{j,k} \right) / MN \right| \tag{17}$$

where ***M*** x ***N*** is size of blur image and deblurred image, after deconvolution operation.

The image quality is estimated by evaluating the average difference value in comparison of output image and input blurred image. In practice, we found that output deblurred image can reach highest quality with minimum value of average difference (AD), and the ringing artifacts in deblurred image are more visible if the average difference is at a large value, as illustrated in Tab. 1 and Fig. 3.The results of deconvolution with different kernels are present in Fig. 4. Figs. 4(c), (g) (j), (n) are output deconvolution with (19x19) kernel in "Bird.jpg", (25x25) kernel in "Fishes.jpg", (11x11) kernel in "Lion.jpg" and (15x15) kernel in "Palace.jpg" respectively. Clearly these images are deblurred well than those that are deblurred with another size of kernel, the ringing artifacts are suppressed in these cases.

Table 1. The value of Average Difference with different size of kernels

PSF Size	"Bird"	"Fishes"	"Lion"	"Building"
11*11	0.0200	0.0293	0.0668	0.4275
13*13	0.0214	0.0394	0.0786	0.3364
15*15	0.0126	0.0501	***0.0128***	***0.1929***
17*17	0.0185	0.0532	0.5243	0.4275
19*19	***0.0043***	0.0552	4.2777	0.3108
21*21	0.0047	0.0247	2.7862	0.4861
23*23	0.0036	0.0263	0.3460	0.7682
25*25	0.0157	***0.0080***	0.6935	1.0469
27*27	0.2444	0.0162	1.0194	1.2087
29*29	0.2894	0.1040	1.2385	1.5126
31*31	0.3148	0.1040	2.3672	1.8504

III. EXPERIMENTAL RESULTS AND COMPARISONS

In this section, we test our approach in different scenarios and compare with some typical blind deconvolution methods: Fergus et al's method (2006), Jia et al's method (2007), Shan et al's method (2008) and Yuan et al's method (2007). We also run Cho et al's method (2011) for image restoration using the kernel estimated by these methods. Cho et al's method (2011) effectively restores even tiny image edges for accurate kernel estimation, but introduces visible ringing artifacts when the kernel estimation error is large. Therefore, it can be used to test the kernel accuracy visually. Yuan et al's result restore from a noisy and blurred image pair is given in Fig. 2(b). For Fergus et al's method, we use release code online and exhaustively tune all options and select different regions in the image to produce the best result. For Jia et al's method, we select patches to minimize the alpha-estimation error. For Shan et al's method, we use the executable online and hand tuned parameters to produce the most visually pleasant results. Fig. 2 shows that all above mentioned blind deconvolution methods are able to produce trajectory-like kernel. In contrast, our kernel is closer to Yuan et al's two image deconvolution results which has been proved to be very accurate. Fergus et al's method and Jia et al's method use standard RL algorithm to recover the image, and thus produce the largest ringing. Shan et al's method reduces the ringing, but suppresses the image details as shown by the closed up views. Cho et al's method using the kernel by Fergus et al's method produces obvious ringing due to the large kernel estimation errors. We found that the kernel estimated by Shan et al's method is accurate enough for the Cho et al's method to suppress the ringing, and the resultant image is visually pleasing. Our approach can produce a high quality result which is comparable to one of Yuan et al's double image deconvolution technique.

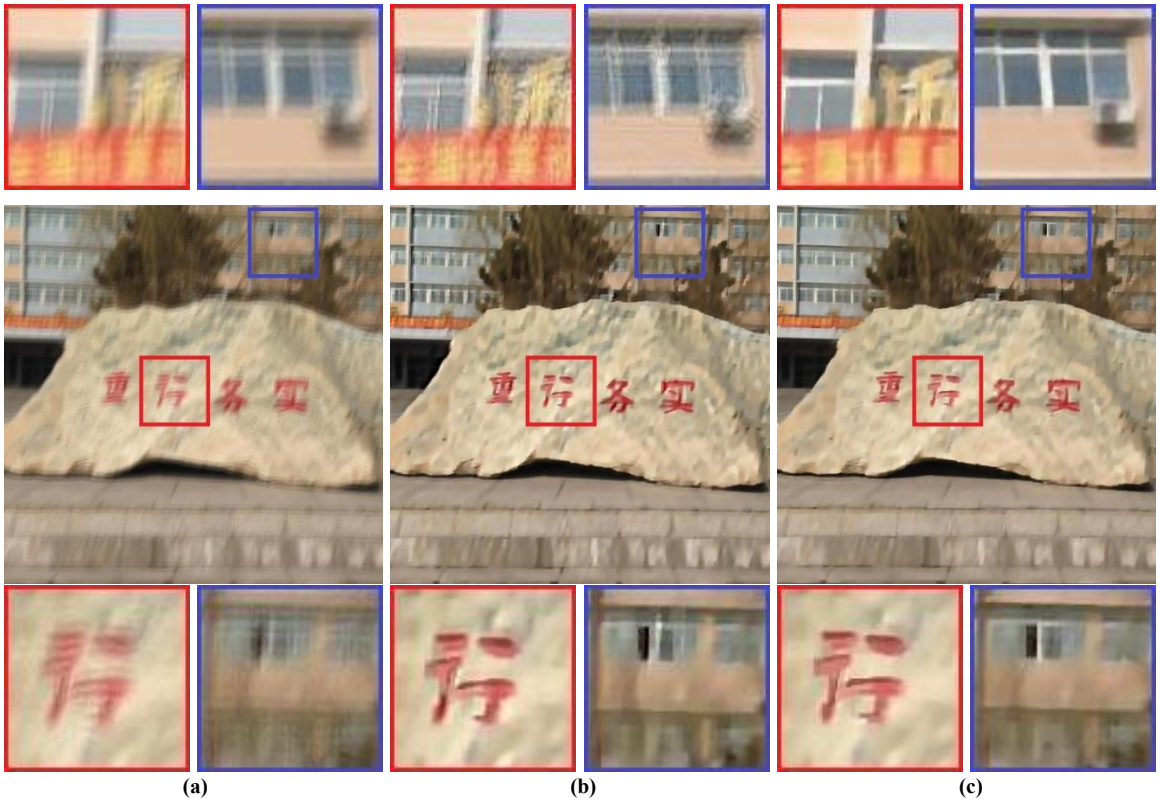

Figure 4. Comparisons between Fergus et al's method (b) and our method (c)

Fig. 6(a) shows an image containing detailed structures, and Fig. 7(a) shows an example lacking highly textured regions. The kernel sizes are 25x25 and 35x35, respectively. Fergus et al's method produces inaccurate kernel for Fig. 6(a) and fails to produce trajectory-like kernel for Fig. 7(a). The kernels by Shan et al's method have good trajectory shapes but are still noisy. In comparison, our kernels are more clean and continuous. We tune the parameters of Shan et al's method to suppress most of the ringing artifacts, but find that many subtle image textures are over-smoothed inevitably. Cho et al's method using Shan et al's kernels recovers more the fine details, such as sail structures on the boat in Fig. 6(c) and the tiny textures on the signboard in Fig. 7(c), but also introduces more unpleasant ringing due to the large kernel noise. Our results preserve almost the same amount of image details, but look much more natural.

Fig. 6(a) shows an image containing detailed structures, and Fig. 7(a) shows an example lacking highly textured regions. The kernel sizes are 25x25 and 35x35, respectively. Fergus et al's method produces inaccurate kernel for Fig. 6(a) and fails to produce trajectory-like kernel for Fig. 7(a). The kernels by Shan et al's method have good trajectory shapes but are still noisy. In comparison, our kernels are more clean and continuous. We tune the parameters of Shan et al's method to suppress most of the ringing artifacts, but find that many subtle image textures are over-smoothed inevitably. Cho et al's method using Shan et al's kernels recovers more the fine details, such as sail structures on the boat in Fig. 6(c) and the tiny textures on the signboard in Fig. 7(c), but also introduces more unpleasant ringing due to the large kernel noise. Our results preserve almost the same amount of image details, but look much more natural.

As far as we know, there are no blind deconvolution methods published to be able to handle such a large blur. Fig. 8(a) is a very challenging example consisting of flat regions and very simple structures. Yuan et al's double image blind deconvolution result is shown in Fig. 8(c). Fergus et al's method fails to estimate trajectory-like kernels. The kernel estimated by Shan et al's method is very noisy as shown in Fig. 8(b), and thus results in unacceptable ringing. The image size of the coarsest scale corresponding to the 3x3 kernel is smaller than our minimum practical size, so we only down-sample the blurred image until it reaches 128x128, and initialize the kernel with Shan et al's kernel. Our result also contain some ringing, but it still of high quality due to our more accurate kernel estimation.

The proposed algorithm and Fergus et al's algorithm are demonstrated with the same size of blur kernel and also have given some other results for comparisons. The input observed images are shown in Figs. 4(a) (first column). The restored images by R. Fergus et al's algorithm are displayed in Figs. 4(b) (second column), and the images restored by our algorithm are shown in Figs. 4(c) (third column) respectively. The image deconvolution is estimated by (19 x 19), (25 x 25) and (11 x 11) size of kernel for from top to bottom row's images, respectively. According to the restoration results, the proposed algorithm can recover the image quite well. Visually, we find that the restored images (third column) are clearer, brighter than those given in Fergus et al's algorithm. The shadow around the main objects are reduced in Fig. 4(b) (R. Fergus et al's algorithm) and those effects have almost disappeared in Fig. 4(c) (our algorithm). The Chinese character in Fig. 4(c) are also clearer than those character in Figs. 4(a) and (b). The shaken effect is also suppressed completely in other pictures in Fig. 4(c).

(a) (b) (c) (d)

Figure 5. Close-up patches of comparison between Fegus et al's method (a, c) and our results (b, d)

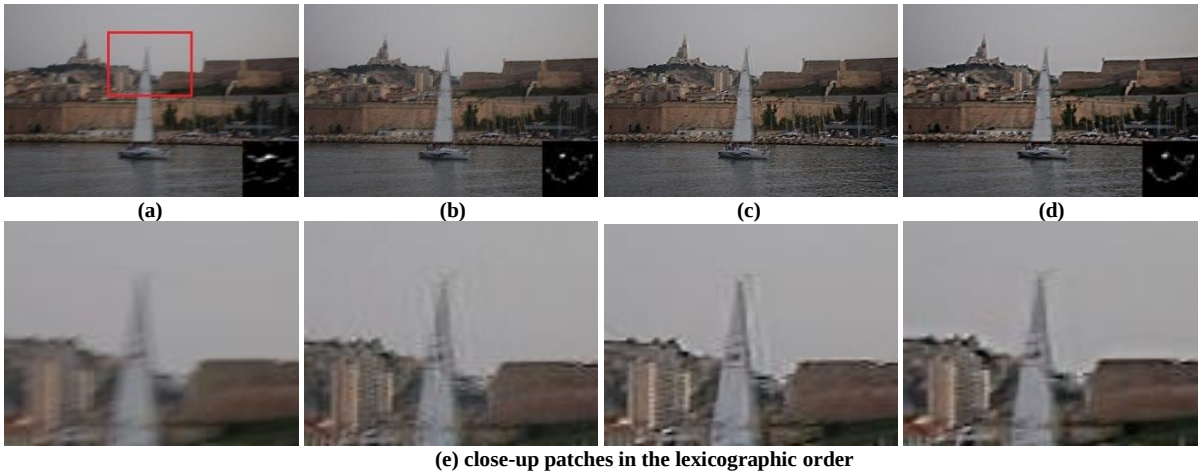

(a) (b) (c) (d)

(e) close-up patches in the lexicographic order

Figure 6. Blurred image, (b) Result by Shan et al., (c) Result by Cho et al. using kernel in (b), (d) Our result, (e) Closed-up patches for (a-d)

(a) (b) (c) (d)

(e) close-up patches in the lexicographic order

Figure 7. Restoration with kernel estimated by Fergus et al., (a) Blurred Image, (b) Result by Shan et al., (c) Result by Cho et al., (d) Our result, (e) Closed-up patches for (a-d)

The improvement of method is exposed in close-up patches of the restored images, which are shown in Fig. 7. The close-up patches of restored images by Fegus et al's method and our method are displayed in Figs. 7(a, c), Figs. 7(b, d) respectively. The edges are well preserved in Fegus et al's method but there has been the severe ringing and noise in output image. When the ringing and noise are reduced significantly (by increasing kernel size), the image details are also reduced. In contrast, our method show the accurate results with reduced ringing and noise in close-up patches, while preserving image edges well. The objects in image as shown in Figs. 7(b, d) are clear and the artifacts such as ringing and noise in the background are reduced significantly with our method. Again it is clear that the proposed algorithm can restore images quite well.

(a) **(b)** **(c)** **(d)**

Figure 8. (a) Blurred image, (b) result by Shan et al., (c) Result by Yuan et al's two image deblurring method, (d) Our result

IV. CONCLUSION

In this paper, we introduced a novel deconvolution algorithm for image restoration. The proposed method can not only increase the accuracy of kernel estimation by using multi-scale approach but also effectively handles the outlier by applying EM based method to deconvolution process. We further demonstrate that by using two multi-scale frameworks and found that our approach produces high quality results from most of shaken images. The methodology is also compared with other previous method in a number of scenarios. In comparison, the experimental results have shown that our method produced an accuracy quality of latent image and suppress most of the ringing artifacts. One limitation of our approach is the computational cost. Processing a mega-pixel image with large kernel will take a long time. Another limitation is that when the observed blurry image is modeled as the convolution of a sharp image with a non-uniform blur kernel, there still exist some artifacts in final deblurred image. We believe that these limitations will be solved by improving the kernel estimation step and developing a geometrically motivated model of non-uniform image blur due to camera shake in future works.

REFERENCES

[1] Caron, J., Namazi, N., Rollins, C. (2002). Noniterative blind data restoration by use of an extracted filter function, Applied Optics 41, 32 (November), pp 68–84.
[2] Chen, J., Yuan, L., Tang, C. K. and Quan L. (2008). Robust dual motion deblurring, In Proc. CVPR.
[3] Cho, S., Wang J., Lee S. (2011), Handling Outliers in Non-Blind Image Deconvolution, IEEE Conf., pp. 495–502.
[4] Cho, S., Matsushita, Y., Lee, S. (2007). Removing non-uniform motion blur from images, In Proc. ICCV 2007, pp. 1–8.
[5] Cho, S. and Lee, S. (2009). Fast motion deblurring. ACM Trans. Graphics (Proc. SIGGRAPH Asia 2009), 28(5):145:1–145:8.

[6] Dabov, K., Foi, A., Katkovnik, V., and Egiazarian, K. (2008). Image restoration by sparse 3D transform-domain collaborative filtering. SPIE Electronic Imaging.
[7] Fergus, R., Singh, B., Hertzbann, A., Roweis, S.T., Freeman, W. (2006). Removing camera shake from a single photograph, ACM T. Graphic., 25, pp. 787–794.
[8] Gupta, A., Joshi, N., Zitnick, C. L., Cohen, M. and Curless, B. (2010). Single image deblurring using motion density functions, In Proc. ECCV.
[9] Harmeling, S., Sra, S., Hirsch, M., Scholkopf, B. (2010). Multiframe blind deconvolution, super-resolution, and saturation correction via incremental EM. In Proc. ICIP 2010, pp. 3313–3316.
[10] Joshi, N. (2008). Enhancing photographs using content-specific image priors. PhD thesis, University of California, San Diego.
[11] Joshi, N., Kang, S. B., Zitnick, C. L. and Szeliski R. (2010). Image deblurring using inertial measurement sensors. ACM Trans. Graphics (Proc. SIGGRAPH 2010), 29(4):30:1–30:9.
[12] Levin, A., Weiss, Y., Durand, F., Freeman, W. T. (2009). Understanding and evaluating blind deconvolution algorithms. CVPR.
[13] Miskin, J., Mackay, D. J. C. (2000). Ensemble Learning for Blind Image Separation and Deconvolution, Adv. in Independent Component Analysis, M. Girolani, Ed. Springer-Verlag.
[14] Shan, Q. , Jia, J., Agarwala, A. (2008). High-quality motion deblurring from a single image, SIG-GRAPH.
[15] Yuan, L., Sun, J., Quan, L., Shum, H.Y. (2008). Progressive inter-scale and intra-scale non-blind image deconvolution, ACM Trans. Graphics.
[16] Michael Hirsch, Christian J, Schuler, Stefan Harmeling, Bernhard Scholkopf (2011). Fast Removal of Non-uniform Camera Shake, Proc. IEEE International Conference on Computer Vision 2011.
[17] Stefan Harmeling, Michael Hirsch, Bernhard Scholkopf (2010). Space-Variant Single-Image Blind Deconvolution for Removing Camera Shake, NIPS Conference 2010.
[18] Li Xu, Jiaya Jia (2010). Two-Phase Kernel Estimation for Robust Motion Deblurring, ECCV 1, volume 6311 of Lecture Notes in Computer Science, page 157-170.Springer
[19] Krishnan, D., Fergus, R (2009). Fast Image Deconvolution using Hyper-Laplacian Priors. Advances in Neural Information Processing Systems, vol. 22, pp 1-9
[20] Osher, S., Rudin, L.I. (1990). Feature-oriented Image Enhancement using Shock Filters. SIAMJournal on Numerical Analysis, vol. 27, pp. 919-940
[21] Levin, A., Fergus, R. Durand, F., Freeman, W.T. (2007). Image and Depth from a Conventional Camera with a Coded Aperture. ACM Trans. on Graph. (SIGGRAPH), vol. 26, pp. 70-77

AUTHORS

Phu Ninh Tran Male, was born in 1980. He received the B.S., M.S. degrees from the Le Qui Don Technical University, Hanoi, Vietnam, in 2004 and 2011, respectively. Now he is currently working in Faculty of Radio-electronic, Le Quy Don Technical University as senior Lecturer. He currently focuses on Blind Deconvolution, Image processing.

Quang Thi Nguyen Male, was born in 1980. He received the B.S., M.S. degrees from the Le Qui Don Technical University, Hanoi, Vietnam, in 2004 and 2011, respectively. Now he is currently working in Faculty of Radio-electronic, Le Quy Don Technical University as senior Lecturer. He currently focuses on Blind Deconvolution, Image processing.

Quang Hieu Dang Male, was born in 1974. He received the B.S., M.S. degrees from the Le Qui Don Technical University, Hanoi, Vietnam, in 1996 and 2001, respectively. Now he is currently working in Integrated System Institute, Le Quy Don Technical University. He currently focuses on Blind Deconvolution, Image processing.

Hong Quang Le Male, was born in 1980. He received the B.S., M.S. degrees from the Le Qui Don Technical University, Hanoi, Vietnam, in 2004 and 2011, respectively. Now he is currently working in Faculty of Missile and Artillery, Vietnam Naval Academy. He currently focuses on Blind Deconvolution, Image processing.